

# An atomistic-based chemophysical environment for evaluating asphalt oxidation and antioxidants

Tongyan Pan · Lu Sun · Qifeng Yu

Received: 3 May 2012 / Accepted: 15 June 2012 / Published online: 8 July 2012  
© Springer-Verlag 2012

**Abstract** Asphalt binders in service conditions are subject to oxidative aging that involves the reactions between oxygen molecules and the component species of bulk asphalt. As a result, significant alterations can occur to the desired physical and/or mechanical properties of asphalt. A common practice to alleviate asphalt aging has been to employ different chemical additives or modifiers as antioxidants. The current state of knowledge in asphalt oxidation and antioxidant evaluation is centered on determining the degradation of asphalt physical properties, mainly the viscosity and ductility. Such practices, although meeting direct engineering needs, do not contribute to the fundamental understanding of the aging and anti-oxidation mechanisms, and thereby developing anti-aging strategies. From this standpoint, this study was initiated to study the chemical and physical bases of asphalt oxidation, as well as the anti-oxidation mechanisms of bio-based antioxidants using the coniferyl-alcohol lignin as an example. A quantum chemistry (QC) based chemophysical environment is developed, in which the various chemical reactions between asphalt component species and oxygen, as well as the incurred physical changes are studied. X-ray photoelectron spectroscopy (XPS) was used to validate the modified and unmodified asphalt models.

**Keywords** Asphalt · Atomistic modeling · Lignin · Oxidative aging · Quantum chemistry · XPS

## Introduction

Asphalt materials are the primary binding and waterproofing material in road pavements and roof shingles. As an organic product from the remains of ancient organisms, asphalt in service however is subject to atmospheric oxidation, which has been the main cause of long-term deterioration of asphalt binders in their end products [1–4]. The complex oxidation reactions involve the various chemicals present in asphalt and atmospheric oxygen molecules and can last throughout the service life of the asphalt-based products.

Chemical composition and the environmental temperature are the primary factors of asphalt oxidation. Asphalts of different origin and distillation methods oxidize differently. Asphalt binder is composed primarily of carbon and hydrogen, with nitrogen and sulfur of lower percentages [4]. Often some trace heavy metals such as vanadium and nickel are also present. These elements combine to form the main fractions of asphalt cement: asphaltenes, saturates, naphthalene and polar aromatics (also known as light and heavy resins, respectively) according to the Corbett's method [5]. The three fractions, each providing different properties of asphalt, chemically and physically interact with each other and form the complex mixture system of asphalt. Asphaltenes and saturates are normally incompatible compounds, and are brought together by aromatics. Asphaltenes are the main contributors of viscosity and therefore hardening effects; and an abundance of aromatics and saturates decrease the ductility and hence elastic effects [4–12]. As for the factor of temperature, most of the aging occurs during the process of making asphalt-based end products, such as asphalt concrete

---

T. Pan (✉) · L. Sun · Q. Yu  
The Catholic University of America,  
620 Michigan Avenue, N.E.,  
Washington, DC 20064, USA  
e-mail: pan@cua.edu

L. Sun  
e-mail: sunl@cua.edu

Q. Yu  
e-mail: yuq@cua.edu

in the intense heat of an asphalt plant [1]. During the short duration of heating, the temperature can reach 135 °C–165 °C. Long-term oxidative aging begins immediately after the end product, such as an asphalt pavement, is put in service, which occurs at a much slower rate than the initial oxidation of asphalt during mixing and production. However, long-term oxidative aging can cause failures as serious as the initial oxidation, including a large increase in stiffness and loss of ductility, and cracking of the end products under thermal and/or load stresses [4].

In general, oxidative hardening of asphalt is believed to be caused by the generation of oxygen-containing polar chemical functionalities on asphalt molecules, which in turn can cause agglomeration among molecules due to increased chemophysical associations such as hydrogen bonding, van der Waals force, and Coulomb force [4–10, 12]. In addition to oxygen-containing functionalities, oxidation can also cause aromatization of certain asphalt molecules that facilitates further agglomeration of asphalt components in ambient conditions [5–10]. However, the systematic study of asphalt oxidation from the chemical perspective has not been seriously attempted due to one underlying challenge in the state of knowledge: the complexity of chemical composition in asphalt, which has naturally led to the lack of an effective tool for studying the manifold chemical reactions involved in asphalt oxidation [3, 8].

Various chemical agents have been studied as potential asphalt antioxidants. The presence of some polymers in asphalt, among various chemical antioxidants, can effectively decrease aging rate and reduce asphalt's temperature susceptibility, such as the use of styrene-butadiene-styrene (SBS) and styrene-butadiene (SBR) in high-volume roadways to increase the high- and low-temperature properties of asphalt and reduce the pavement's tendency to form ruts or crack [13]. There are many polymers that have shown anti-oxidation abilities for asphalt; however, in the state of practices none of them truly demonstrates satisfactory in-situ anti-oxidative performance [14]. As such, the identification of an effective antioxidant of asphalt binder is of great benefit to the asphalt-related industries.

Among the polymers once evaluated as antioxidants for asphalt, wood lignin has shown anti-oxidation effectiveness [15]. When a seven percentage by weight is added in asphalt, wood lignin significantly slows down its oxidation. Being one of the most abundant organic polymers on Earth (right after cellulose), lignins constitute 30 % of non-fossil organic carbon and from a quarter to a third of the dry mass of wood [16]. Lignin as a biopolymer is a cross-linked three-dimensional hydrophobic and aromatic molecule. The degree of polymerization in lignin is difficult to measure, since it is fragmented during extraction and the molecule consists of various types of substructures that appear to repeat in a haphazard manner. Although different forms of lignin have been described depending on the means of isolation, there are three monolignol monomers in the form of a benzene ring

with a tail of three carbons, methoxylated to various degrees: p-coumaryl alcohol, coniferyl alcohol, and sinapyl alcohol [16]. The coniferyl alcohol is the main monomer unit that makes up the lignin in softwood. These lignols are incorporated into lignin in form of the phenylpropanoids p-hydroxyphenyl, guaiacyl, and syringal, respectively [16].

As an asphalt antioxidant, the effects of lignins are derived from the scavenging action of their phenolic structures on oxygen containing free radicals [17]. Phenolic structures are benzene rings with attached hydroxyl groups. Benzene rings are six carbon structures with each carbon sharing a single and double covalent bond to another carbon. In a phenolic group, there can be one or more hydroxyl groups attached to the benzene ring. The ability of phenolic compounds to be antioxidants is the functional group's ability to neutralize free radicals [18]. A phenol can neutralize a free radical by donating either a proton or an electron [17]. Because of its structure, a phenol is able to do both while remaining relatively stable. Lignin contains a large amount of phenolic groups, making it an effective antioxidant [18]. Many factors affect the antioxidant ability of lignin, of which the source of biological origin is the most prominent factor [17, 18]. Each plant is biologically and chemically different; therefore, the lignin obtained from them will be different. The extraction method is also very important in determining a lignin's antioxidant ability. Lignin can be extracted from plant material by chemicals such as ethanol, acetone, acetic acid, methanol, and propanol, which produce lignins of different antioxidant abilities [17].

It is noteworthy that when lignin is studied as an asphalt antioxidant, it can also become oxidized when exposed to oxygen or atmosphere, particularly at raised temperature. At the temperature of  $\geq 150$  °C, oxidation of lignins could be significant [19]. Based on a comprehensive study of oxidation of lignins from different sources (150 °C in oxygen for 4 hours), the combined gas-liquid chromatography and a sequential methylation technique indicated the presence of a larger number of products, including different acids of low molecular weights (e.g., formic acid, two-carbon-atom acids, and some three-carbon-atom and four-carbon-atom acids), and various phenolic compounds such as vanillin, syringaldehyde, and p-hydroxybenzaldehyde as the methyl ethers and carboxy-containing compounds as the methyl esters or methyl ether esters [19]. According to Bryan [20], oxygen in the early stages of oxidation is necessary to break lignin polymer into smaller molecular fragments. Notably, the level of temperature around 150 °C is close to those for producing many asphalt products such as asphalt mixtures for pavements, and might be of significance when lignin is evaluated as an asphalt antioxidant in such products.

To form a more fundamental understanding of the phenomenon of asphalt oxidation and to evaluate the effectiveness of bio-based antioxidants, a research study was recently conducted in which the molecular-scale mechanisms of asphalt oxidation

and anti-oxidation by lignins were studied in an atomistic-based chemophysical environment. This manuscript presents the results of the study, with a focus on reporting the development of quantum chemistry (QC) based chemophysical environment (in forms of a series of atomistic models), validation of the models, and utilization of the models in studying asphalt oxidation and specific lignin as a potential antioxidant.

## Methods

### Quantum chemistry perspective of asphalt oxidation

Although a fundamental understanding of asphalt oxidation is highly desired when dealing with the problems related to asphalt aging, this task cannot be readily accomplished within the frame of traditional organic or polymer chemistry that has centered on experimenting with bulk asphalt using different devices. The past few decades has seen significant advances made in using spectroscopic techniques for characterizing molecular and atomic phenomena that involve essentially the transfer of electrons [21–26]. Since the oxidation of asphalt is mainly a chemical process, an approach capable of simulating electron-transfer processes is desired. In this study, quantum chemistry (QC) is resorted to as such an approach. In recent years, the efforts made in atomic-level description of phenomena have been accelerated by the availability of powerful computers and parallel computing methods, advances in statistical mechanics and new experimental data. The QC-based methods today are readily implemented using different computer-based programs, of which the dominant one is the density functional theory (DFT) [27].

Even though recent computing capacity has significantly improved the speed of QC computation that enables predicting accurately the geometries and vibrational energies, extensive use of QC computation today is still limited to small atomic/molecular systems and therefore is not practical for studying asphalt oxidation. From this standpoint, it is necessary to have an accurate force-field based method that enables quick evaluation of inter-atomic bonding and forces. Such a first principle based force-field method has the advantage of being able to simulate chemical reactions while obtaining fast computation speed as traditional force field methods do, and therefore is highly desired for simulating asphalt oxidation that involves thousands of atoms for a realistic simulation.

### Fundamental of reactive force field for asphalt oxidation

One first principle based force-field method is the *reactive force field* (ReaxFF) developed by van Duin et al. [24] that since advent has been parameterized and implemented to a variety of materials and processes, including hydrocarbon reactions, transition-metal-catalyzed nanotube formation, and high-energy materials. Recently ReaxFF has been extended to more

materials including various metals, ceramics, silicon, and polymers, and is now used as a general tool for chemical simulations. A reactive force field of a C-H-O-S system as originally developed by van Duin et al. [24, 28] is re-evaluated and used in this study to simulate the oxidation of asphalt in exposure to oxygen.

The overall energy of the C-H-O-S ReaxFF contains a series of energy contributions per Eq. 1, all determined using QC. The actual number of energy contributions of a ReaxFF system depends on the type of chemical species and processes to be modeled. The ReaxFF for simulating asphalt oxidation in an oxygen environment involves complex chemical reactions between the five element species of asphalt and external oxygen.

$$E_{system} = E_{bond} + E_{val} + E_{tors} + E_{H-bond} + E_{vdWaals} + E_{Coulomb} \tag{1}$$

In Eq. 1, the bond energy  $E_{bond}$  describes the chemical energy between each pair of bonded atoms. Valence angle energy  $E_{val}$  accounts for the energy contribution from valence angle; the torsion rotation energy term  $E_{tors}$  is formulated in a way that the torsion angle energy gradually develops with the changes in torsion angle  $\omega_{ijk}$  and bond order even when the bond order approaches zero or increases to exceed 1; van der Waals interactions energy  $E_{vdWaals}$  accounts for the van der Waals interactions; and the term Coulomb interactions energy  $E_{Coulomb}$  between all atom pairs is included to adjust energy variation due to orbital overlap between atoms at close distances.

The fundamental ReaxFF assumption is that the bond order  $BO'_{ij}$  between a pair of atoms is dependent on the interatomic distance  $r_{ij}$  according to Eq. 2, in which the parameter  $r_0$  is the bond radius and the series of parameters  $p_s$  describe the bond order. In calculating bond orders, ReaxFF distinguishes between contributions from  $\sigma$  bonds,  $\pi$  bonds, and  $\pi\pi$  bonds. The bond orders  $BO'_{ij}$  are updated in each time step. The energy of the system is finally determined by summing up all the energy contributions per Eq. 1. The three pairs of parameters:  $p_{bo,1}$  and  $p_{bo,2}$ ,  $p_{bo,3}$  and  $p_{bo,4}$ , and  $p_{bo,5}$  and  $p_{bo,6}$  in Eq. 2 correspond to the orders of the  $\sigma$  bond, the first  $\pi$  bond, and the second  $\pi\pi$  bond, respectively, of which the values are given in Table 1. The values of the exponential terms is unity below a particular interatomic distance  $r_0$  and negligible at a longer distance. The bond energy is calculated from the bond order  $BO'_{ij}$ .

$$BO'_{ij} = BO_{ij}^{\sigma} + BO_{ij}^{\pi\pi} = \exp \left[ P_{bo1} \cdot \left( \frac{r_{ij}}{r_0} \right)^{Pbo2} \right] + \exp \left[ P_{bo3} \cdot \left( \frac{r_{ij}}{r_0} \right)^{Pbo4} \right] + \exp \left[ P_{bo5} \cdot \left( \frac{r_{ij}}{r_0} \right)^{Pbo6} \right] \tag{2}$$

The connectivity related terms in Eq. 1 such as the bond energy, valence angle and torsion angle energy terms are also bond order dependent and will disappear upon bond dissociation. This feature of ReaxFF ensures a smooth transition of the energy and force from a bonded system to a non-bonded system. In addition to the valence interactions which depend on overlap, there are repulsive interactions at short interatomic distances due to Pauli principle orthogonalization and attraction energies at long distances due to dispersion. These interactions, comprised of van der Waals and Coulomb forces, are included for all atom pairs, thus avoiding awkward alterations in the energy description during bond dissociation. In this respect, ReaxFF is similar in spirit to the central valence force fields used earlier in vibrational spectroscopy. The following sections introduce these energy contribution terms.

### Bond energy

$E_{bond}$  of the C-H-O-S system was determined according to Eq. 3.  $D_e$  and  $p_{be,1}$  and  $p_{be,2}$  are bond parameters. Upon the dissociation of a bond, the bond order  $BO'_{ij}$  approaches zero making the bond energy term  $E_{bond}$  disappear (Eq. 3). To simulate oxidation of asphalt, the energy contributions developed by van Duin et al. [24, 28] are used to determine the overall system energy—hence the ReaxFF potential function—for the atomic-level modeling of asphalt oxidation, with the parameters given in Table 1.

$$E_{bond} = -D_e \cdot BO'_{ij} \cdot \exp[p_{be1}(1 - (BO'_{ij})^{p_{be2}})] \quad (3)$$

### Valence angle energy

$E_{val}$  was determined according to Eq. 4. Just like bond energy, it is important that the energy contribution from valence angle term goes to zero as the bond orders in the valence angle goes to zero. Equation 4 determines the energy associated with deviations in valence angle  $\Theta_{ijk}$  from its equilibrium value  $\Theta_o$ . The term  $f_1(BO)$  per Eq. 4a ensures that the valence angle energy contribution disappears smoothly during bond dissociation. Equation 4b deals with the effects of over/under coordination in central atom  $j$  on the valence angle energy. Atom undercoordination/overcoordination parameter  $\Delta_j$  is defined for atoms as the difference between the total bond order around the atom and the number of its bonding electrons valence. The equilibrium angle  $\Theta_o$  for  $\Theta_{ijk}$  depends on the sum of  $\pi$ -bond orders around the central atom  $j$  and changes from around  $109.47^\circ$  for  $sp^3$  hybridization ( $\pi$ -bond=0) to  $120^\circ$  for  $sp^2$  ( $\pi$ -bond=1) to  $180^\circ$  for  $sp$  ( $\pi$ -bond=2) based on the geometry of the central atom  $j$  and its neighbors. Table 2 lists the parametric values used to determine the valence angle energy  $E_{val}$ .

$$E_{val} = f_1(BO_{ij}) \cdot f_1(BO_{jk}) \cdot f_2(\Delta_j) \cdot \{p_{val1} - p_{val1} \exp[-p_{val2}(\Theta_o(BO) - \Theta_{ijk})^2]\} \quad (4a)$$

$$f_1(BO_{ij}) = 1 - \exp(-BO_{ij}^{p_{val3}}) \quad (4b)$$

$$f_2(\Delta_j) = \frac{2 + \exp(\Delta_j)}{1 + \exp(\Delta_j) + \exp(-p_{val4} \cdot \Delta_j)} \quad (4c)$$

**Table 1** ReaxFF parameters for determining bond order and  $E_{bond}$  of asphalt (a C-H-O-S system)

Bond	$D_e$ (kcal/mol)	$p_{be,1}$	$p_{be,2}$	$p_{bo,1}$	$p_{bo,2}$	$p_{bo,3}$	$p_{bo,4}$	$p_{bo,5}$	$p_{bo,6}$
C-C	145.4070	0.2176	-0.1940	5.9724	1.0000	8.6733	1.0000	-0.7816	0.3217
C-H	167.1752	-0.4421	1.0000	8.5445	0.0000	0.0000	1.0000	0.0000	0.5969
H-H	188.1606	-0.314	1.0000	5.7082	0.0000	0.0000	1.0000	0.0000	0.6816
C-O	171.0470	0.36	-0.2660	5.0637	0.0000	7.4396	1.0000	-0.1696	0.3796
O-O	90.2465	0.995	-0.1850	6.2396	1.0000	7.5281	1.0000	-0.2435	0.9704
H-O	216.6018	-0.4201	1.0000	5.9451	0.0000	0.0000	1.0000	0.0000	0.9143
C-S	128.9942	0.1035	-0.2398	5.6731	1.0000	8.1175	1.0000	-0.5211	0.6000
H-S	151.5159	-0.4721	1.0000	7.0050	1.0000	0.0000	1.0000	0.0000	0.6000
O-S	100.0000	0.5563	-0.4577	7.1145	1.0000	12.7569	1.0000	-0.4038	0.6000
S-S	96.1871	0.0955	-0.2373	6.4757	1.0000	9.7875	1.0000	-0.4781	0.6000

**Table 2** Parameters for determining valence angle energy

Angle atoms	$\Theta_0$ (degree)	$p_{val,1}$ (kcal/mol)	$p_{val,2}$ (1/radian <sup>2</sup> )	$p_{val,3}$	$p_{val,4}$
C-C-C	70.0265	13.6338	2.1884	0.1676	1.0400
C-C-H	69.7786	10.3544	8.4326	0.1153	1.0400
H-C-H	74.6020	11.8629	2.9294	0.1367	1.0400
C-H-H	0.0000	0.0000	6.0000	0.0000	1.0400
C-H-C	0.0000	3.4110	7.7350	0.0000	1.0400
H-H-H	0.0000	27.9213	5.8635	0.0000	1.0400
C-C-O	72.9588	16.7105	3.5244	1.1127	1.1880
O-C-O	80.0708	45.0000	2.1487	1.1127	1.1880
H-C-O	66.6150	13.6403	3.8212	0.0755	1.0500
C-O-C	79.1091	45.0000	0.7067	0.6142	1.0783
C-O-O	83.7151	42.6867	0.9699	0.6142	1.0783
O-O-O	80.0108	38.3716	1.1572	0.6142	1.0783
C-O-H	78.1533	44.7226	1.3136	0.1218	1.0500
H-O-O	84.1057	9.6413	7.5000	0.1218	1.0500
H-O-H	79.2954	26.3838	2.2044	0.1218	1.0500
C-H-O	0.0000	0.0019	6.0000	0.0000	1.0400
C-H-S	0.0000	0.0019	6.0000	0.0000	1.0400
O-H-O	0.0000	0.0019	6.0000	0.0000	1.0400
H-H-O	0.0000	0.0019	6.0000	0.0000	1.0400
C-C-S	74.9397	25.0560	1.8787	0.0559	1.0400
C-S-C	86.9521	36.9951	2.0903	0.0559	1.0400
H-C-S	74.9397	25.0560	1.8787	0.0000	1.0400
C-S-H	86.1791	36.9951	2.0903	0.0000	1.0400
C-S-S	85.3644	36.9951	2.0903	0.0559	1.0400
H-S-H	93.1959	36.9951	2.0903	0.0000	1.0400
H-S-S	84.3331	36.9951	2.0903	0.0000	1.0400
H-H-S	0.0000	0.0019	6.0000	0.0000	1.0400

### Torsion rotation energy

$E_{tors}$  is a term defined to reflect the energy changes due to the changes in torsion angle  $\omega_{ijk}$  and bond order  $BO'$  as the bond order varies from zero to above one. This is given in Eq. 5 and

5a-b.  $\Theta_{ijk}$  and  $\Theta_{jkl}$  are valence angles.  $\Delta$  is the atom under-coordination/overcoordination parameter. Parameters  $p_{tor3}$  and  $p_{tor4}$  in Eq. 5b equal zero for the specific types of elements in this study. Table 3 lists the values of parameters  $V_1$ ,  $V_2$  and  $p_{tor}$  used to determine the torsion rotation energy  $E_{tors}$ .

$$E_{tors} = f_3(BO_{ij}, BO_{jk}, BO_{kl}) \cdot \sin \Theta_{ijk} \cdot \sin \Theta_{jkl} \cdot \left[ \frac{1}{2} V_1 \cdot \exp \left\{ p_{tor} \cdot (BO_{jk} - 1 + f_4(\Delta_i, \Delta_k))^2 \right\} \cdot (1 - 2 \cos \omega_{ijkl}) + \frac{1}{2} V_2 (1 + \cos 3\omega_{ijkl}) \right] \quad (5)$$

$$f_3(BO_{ij}, BO_{jk}, BO_{kl}) = [1 - \exp(BO_{ij})] \cdot [1 - \exp(BO_{jk})] \cdot [1 - \exp(BO_{kl})] \quad (5a)$$

$$f_4(\Delta_j, \Delta_k) = \frac{2 + \exp(-\Delta_j - \Delta_k)}{1 + \exp(-\Delta_j - \Delta_k) + \exp(\Delta_j + \Delta_k)} \quad (5b)$$



**Table 3** Parameters for determining torsion rotation energy (X represents any of the elements C, H, O, and S)

Torsion angle	$V_2$ (kcal/mol)	$V_3$ (kcal/mol)	$p_{tor}$
C-C-C-C	23.2168	0.1811	-4.6220
C-C-C-H	45.7984	0.3590	-5.7106
H-C-C-H	44.6445	0.3486	-5.1725
X-C-H-X	0.0000	0.0000	0.0000
X-H-H-X	0.0000	0.0000	0.0000
X-C-O-X	16.7344	0.5590	-3.0181
X-H-O-X	0.1000	0.0200	-2.5415
X-O-O-X	68.9706	0.8253	-28.4693
X-C-C-X	0.9305	0.0000	-24.2568
X-C-S-X	30.3435	0.0365	-2.7171
X-S-S-X	-42.7738	0.1515	-2.2056
X-H-S-X	0.0000	0.0000	0.0000

### Hydrogen bond interactions

Equation 6 described the bond-order dependent hydrogen bond term for an X-H—Z system as incorporated in ReaxFF.

$$E_{vdWaal} = D_{ij} \cdot \left\{ \exp \left[ \alpha_{ij} \cdot \left( 1 - \frac{f_5(r_{ij})}{r_{vdW}} \right) \right] - 2 \cdot \exp \left[ \frac{1}{2} \cdot \alpha_{ij} \cdot \left( 1 - \frac{f_5(r_{ij})}{r_{vdW}} \right) \right] \right\} \quad (7)$$

$$f_5(r_{ij}) = \left[ r_{ij}^{PvdW1} + \left( \frac{1}{\gamma_w} \right)^{PvdW1} \right]^{\frac{1}{PvdW1}} \quad (7a)$$

### Coulomb interactions energy

$E_{Coulomb}$  is considered between all atom pairs. To adjust for orbital overlap between atoms at close distances a shielded Coulomb potential  $E_{Coulomb}$  is used (see Eq. 8).

$$E_{Coulomb} = C \cdot \frac{q_i \cdot q_j}{\left[ r_{ij}^3 + (1/\gamma_{ij})^3 \right]^{1/3}} \quad (8)$$

Atomic charges are calculated using the electron equilibration method [29, 30]. The initial values for the electron equilibration method parameters ( $\eta$ ,  $\chi$ , and  $\gamma$ ) listed in

**Table 4** Parameters for hydrogen bond interactions energy

Hydrogen bond	$r_{hb}^o$	$p_{hb1}$	$p_{hb2}$	$p_{hb3}$
O-H-O	2.0431	-6.6813	3.5000	1.7295
O-H-S	2.6644	-3.9547	3.5000	1.7295
S-H-O	2.1126	-4.5790	3.5000	1.7295
S-H-S	1.9461	-4.0000	3.5000	1.7295

**Table 4** lists the values of parameters  $r_{hb}^o$ ,  $p_{hb1}$ ,  $p_{hb2}$ , and  $p_{hb3}$  used to determine the torsion rotation energy  $E_{Hbond}$ .

$$E_{Hbond} = p_{hb1} \cdot [1 - \exp(p_{hb2} \cdot BO_{XH})] \cdot \exp \left[ p_{hb3} \left( \frac{r_{hb}^o}{r_{HZ}} + \frac{r_{HZ}}{r_{hb}^o} - 2 \right) \right] \cdot \sin^8 \left( \frac{\Theta_{XHZ}}{2} \right) \quad (6)$$

### Van der Waals interactions energy

$E_{vdWaal}$  accounts for the van der Waals interactions using a distance-corrected Morse-potential given in Eq. 7. By including a shielded interaction (Eq. 7a), excessively high repulsions between bonded atoms (1-2 interactions) and atoms sharing a valence angle (1-3 interactions) are avoided.  $D_{ij}$  is the basic energy term of an atomic pair;  $r_{vdW}$  is the van der Waal radius. The parameter  $\alpha_{ij}$  is set to be 1 for the elements of this study. The other parameters for  $E_{vdWaal}$  are given in Table 5.

Table 6 were determined by Njo et al. [31]. The optimization parameter  $\gamma_{ij}$  in Eq. 8 is included for orbital overlap correction in the electron equilibration method.

### Atomistic modeling of asphalt oxidation

Petroleum asphalt is composed of different chemical elements, including carbon (~85 %), hydrogen (~11 %), and some trace species such as sulfur (1 – 5 %), nitrogen (0 – 1.1 %), oxygen (0.2 – 0.8 %), vanadium (4 – 1400 ppm), and nickel (0.4 – 110 ppm) [32]. Bulk asphalt consists of molecules with different structures formed by atoms of these chemical species. Like in general organic substances, structures of the asphalt molecules are more important than the amount of each element present. Some heteroatoms, i.e., sulfur, nitrogen, oxygen, are attached to carbon atoms in

**Table 5** Parameters for determining van der Waals interaction energy

Atom units	$D_{ij}$ (kcal/mol)	$r_{vdW}$ (Å)	$\gamma_w$	$\alpha_{ij}$	$PvdW1$
C	0.1818	1.8857	2.0784	9.5928	1.5591
H	0.0600	1.603	4.4187	9.3951	1.5591
O	0.088	1.9741	7.7719	10.219	1.5591
S	0.2099	2.0677	4.9055	9.9575	1.5591

**Table 6** Parameters for determining Coulomb interactions energy

Atom type	$\eta$ (eV)	$\chi$ (eV)	$\gamma$ (Å)
C	6.9235	5.7254	0.8712
H	9.8832	3.8196	0.7625
O	7.8386	8.500	1.0804
S	8.2545	6.500	1.0336

different configurations, forming different polar molecules or functional groups due to imbalance of electrochemical forces which are weaker than the primary chemical bond—the covalent bond that holds atoms within asphalt molecules. Molecular interactions among the polar molecules of asphalt are the primary mechanism of agglomerations that strongly influence the physical properties and macroscopic performance of asphalt. Usually a small amount of polar molecules can have a great effect on most engineering behavior of asphalt, such as the resistance to binder-aggregate stripping that in general is believed to be controlled by the adsorption of polar molecules to the surface of mineral aggregates [9, 12].

It is therefore important to maintain a proper balance among the different functional groups in durable and resistant asphalts against oxidative aging [21]. A classic method for separating asphalt into different functional groups is per their solubilities in a series of organic solvents, supplemented with chromatographic analyses (namely, the Corbett method) [5, 12]. To study the oxidation of asphalts in their service conditions, a typical petroleum asphalt can be divided in three representative functional groups: asphaltenes (relatively large molecules insoluble in straight-chain alkanes such as n-heptane or n-pentane), resins (naphthene aromatics—alkane-soluble and elute in aromatic solvents such as benzene, and polar aromatics—alkane-soluble and elute in more polar solvents, such as an aromatic/alcohol mixture), and oils or saturates (molecules that elute immediately in n-heptane) [5, 12]. The resin and oil portions together also are known as maltenes or petrolenes. Asphaltenes, with higher molecular weight and polarity than resins and saturates, if not properly dispersed by the resinous components of maltenes can cause reduced asphalt compatibility and asphalt durability thereby [5, 12].

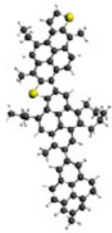
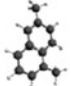

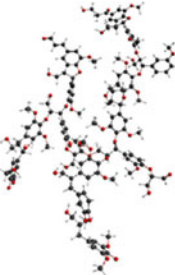

To model asphalt oxidation and the anti-oxidation mechanisms of lignins, a bulk asphalt model is made by mixing a portion of each component functional groups under general service conditions. The bulk asphalt model was originally proposed by Zhang and Greenfield in strict accordance to a real asphalt type [33]. The normal-docosane (n-C<sub>22</sub>H<sub>46</sub>), a saturated aliphatic hydrocarbon with the highest concentration in the speciation reported by Kowalewski et al. [34] was selected to represent the saturate/oil portion of asphalt. Its melting point  $T_m=44$  °C and boiling point  $T_b=369$  °C are

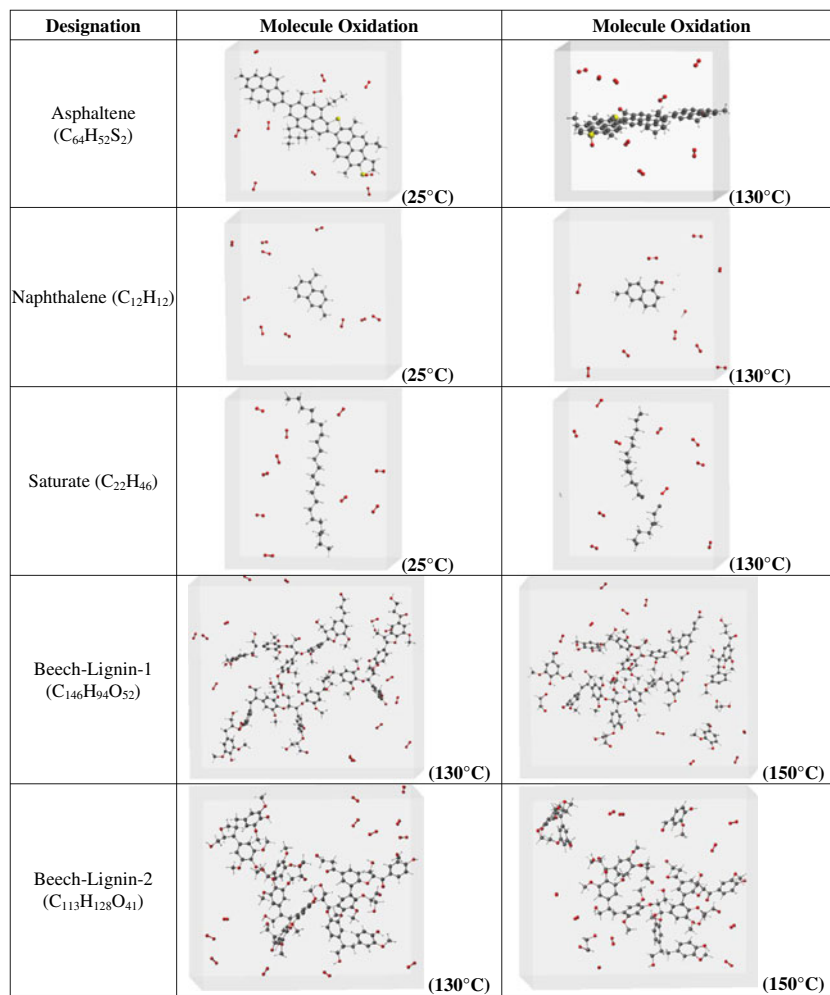
consistent with the waxy component of asphalt. An asphaltene component of asphalt taken from the NMR studies by Artok et al. [35], i.e., C<sub>64</sub>H<sub>52</sub>S<sub>2</sub>, was adopted to represent a portion of the asphaltene molecules. This asphaltene molecule contains a moderate-size aromatic core and a few branches that represent a statistically average asphaltene molecule in general bulk asphalt. For the resin group, the 1,7-dimethylnaphthalene with the number of aromatic rings and side chains intermediate between that of saturates and asphaltenes was selected, that resembles some asphalt molecules depicted earlier [36]. The lignin used for this study was from a commercial source, i.e., the coniferyl alcohol as the main monomer unit of lignins in softwood. The coniferyl-alcohol lignin contains large amounts of phenol structures, giving it antioxidant ability. The ball-stick schemes of the selected asphalt and lignin molecules are shown in Table 7.

Thermodynamics and kinetics are two distinct aspects of a chemical reaction. While thermodynamics describes the possibility and direction of a reaction in terms of the free energy,  $\Delta G$ , released or consumed during a chemical reaction; kinetics concerns how fast the chemical reaction can reach equilibrium, i.e., the rate of the reaction, as influenced by factors of reaction condition such as the temperature and concentrations of reactants. The thermodynamics aspect of asphalt oxidation in this study is evaluated by observing the oxidation behavior of the individual asphalt molecules in a domain of oxygen molecules all at the same concentration. The kinetics of asphalt oxidation depends on factors such as asphalt composition, products formed in oxidation, reaction temperature, oxygen partial pressure, and other chemophysical effects of the system. Accordingly, the kinetics of the different molecular species was evaluated by studying the bulk asphalt model oxidized under the same condition, i.e., at one standard atmospheric (1 ATM) pressure (oxygen only) and 130 °C or 150 °C using the fractions shown in Table 7.

With the selected representative molecules of asphalt and lignin, a series of single-molecule models—one for each representative molecule (see Fig. 1), and a bulk asphalt model (Figs. 2a, c, and e) were developed, to study the thermodynamic and kinetic aspects of the oxidation/anti-oxidation of asphalt and lignin molecules. For the bulk asphalt model, the coniferyl-alcohol lignin was mixed with the asphalt at 130 °C, and then subject to two different levels of temperature, 130 °C and 150 °C, to evaluate its anti-oxidation effect. Chemical functionality developed in asphalt at 130 °C is similar to that develop during normal pavement aging at ambient temperatures [37–39]. Also, oxidation of asphalts in exposure to 100 % oxygen at 1 ATM is believed to be equivalent to that under the 300 psi atmospheric pressure (such as in a Pressure Aging Vessel (PAV)), or that of five or more years in pavements [40]. As such, three oxidation conditions are evaluated in this study: 1) temperature of 25 °C and one ATM, 2) temperature=

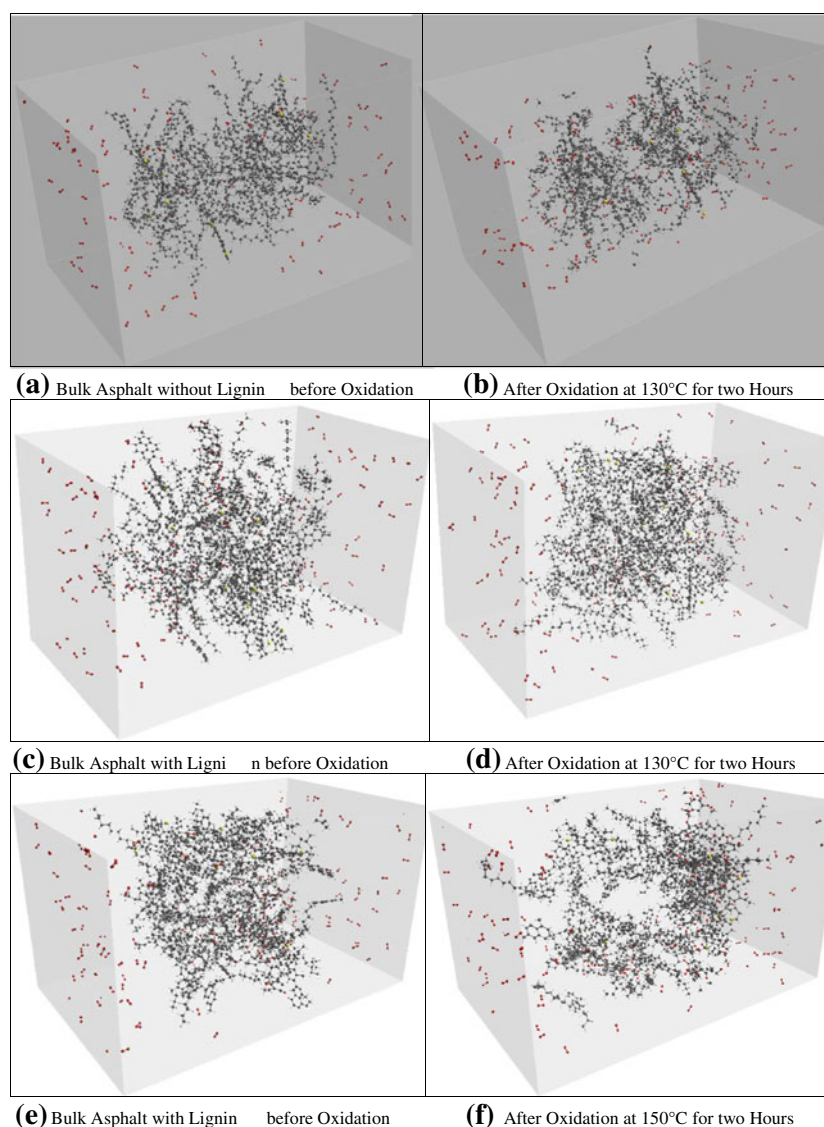
**Table 7** Molecules included in the unmodified and lignin-modified asphalt model

Items	Asphaltene (C <sub>64</sub> H <sub>52</sub> S <sub>2</sub> )	Naphthalene (C <sub>12</sub> H <sub>12</sub> )	Saturate (C <sub>22</sub> H <sub>46</sub> )	Beech-Lignin-1 (C <sub>146</sub> H <sub>94</sub> O <sub>52</sub> )	Beech-Lignin-2 (C <sub>113</sub> H <sub>128</sub> O <sub>41</sub> )
Molecular Structure					
Number of Molecule in Unmodified Asphalt	5	27	41	0	0
Number of Molecule in Modified Asphalt	5	27	41	1	1
Mass Percentage in Unmodified Asphalt	20.7	19.7	59.6	0	0
Mass Percentage in Modified Asphalt	17.8	16.9	51.1	8.0	6.2

**Fig. 1** Thermodynamics study of model asphalt and lignin molecules (1 ATM oxygen pressure, 10 hours)



**Fig. 2** Oxidation of unmodified and lignin-modified bulk asphalts at 130 °C and 150 °C, **a** bulk asphalt without lignin before oxidation; **b** after oxidation at 130 °C for two hours; **c** bulk asphalt with lignin before oxidation; **d** after oxidation at 130 °C for two hours; **e** bulk asphalt with lignin before oxidation; **f** after oxidation at 150 °C for two hours



130 °C and one ATM, and 3) temperature of 150 °C and one ATM. In each condition, in addition to the asphalt and/or lignin molecules only oxygen molecules are included that are separated at an average distance of 1.2 nm (equal to the average air molecule distance at 1 ATM). The use of 1 ATM pressure for modeling is important for studying the escape of existing small-molecule-weight components of asphalt or newly generated ones during asphalt oxidation from bulk asphalt, which might be an important mechanism contributing to asphalt hardening.

The overall mixture composition, i.e., the relative amounts of the three ingredient functional groups used for making the bulk asphalt, was determined based on the measurements by Storm et al. [41], who applied NMR to asphalt fractions separated by the common alkane precipitation method (heptane used) and identified the balance among aromatic and alkane carbons in the asphaltene, resin, and saturate mixtures through the different peak positions of different kinds of carbon

atoms. An asphaltene fraction of 19.6 wt% was selected in this study, which is close to the 22 wt% reported by Storm et al. [41]. The coniferyl-alcohol lignin is 23 wt% in modified asphalt.

As such, each ReaxFF model contains an individual (for thermodynamic study) or a number (for kinetics study) of the saturate, resin, asphaltene and lignin molecules, forming a domain embedded in oxygen molecules (see Fig. 1 for the single-molecule models, and Fig. 2 for the bulk asphalt model). The bulk asphalt was packed to a density of 1000 kg/m<sup>3</sup> prior to adding oxygen molecules into the modeled domain, a typical value for asphalts at ambient conditions. The ReaxFF models were run at a Velocity Verlet plus Berendsen ensemble [42, 43] at a time step of 0.25 femtoseconds (fs) using a parallel computing algorithm developed based on the message-passing interface (MPI) standard. The Virginia Tech's suite of high performance computers—System X, a supercomputer comprising 1100 Apple PowerMac G5 cluster nodes and capable of running

at 12.25 Teraflops was used for the computation. Each ReaxFF model was kept running until the oxidation equilibrium is reached, with no more new species observed for one hour. The modified and unmodified asphalt models after oxidation are also shown in Fig. 2.

#### Validation of the atomistic model

X-ray photoelectron spectroscopy (XPS) as a powerful surface technique was used in this study for determining and thereby validating the oxidative aging of asphalt binders and the anti-oxidation performance of lignin, following well established procedures in which a sufficiently thin sample (e.g., a few  $\mu\text{ms}$ ) was prepared and oxidized with uniform level of oxidation throughout the entire depth of the sample in a relatively short period of time at 130 °C [44–47]. Specifically, XPS was used to determine and compare the amounts of generated functional groups before and after asphalt oxidation.

XPS analysis is based on the photoelectric effect of ejected electrons from the surface of a sample in exposure to electromagnetic radiation of sufficient energy. Electrons emitted have characteristic kinetic energies proportional to the energy of the radiation, according to Eq. 9, in which  $K_E$  is the kinetic energy of the electron,  $h$  is Planck's constant,  $\nu$  is the frequency of the incident radiation,  $E_b$  is the ionization or binding energy, and  $\varphi$  is the work function—a constant dependent on the X-ray photoelectron spectrometer used. In an XPS analysis, a level of energy radiation is used to expel core electrons from a sample, and the kinetic energies of the resulting core electrons are measured. Using Eq. 9 with the kinetic energy  $K_E$  and known frequency  $\nu$  of radiation, the binding energy  $E_b$  of the ejected electron can be determined. By Koopman's theorem, which states that binding or ionization energy is equivalent to the negative of the orbital energy, the energy of the orbital from which the electron originated can be determined. These orbital energies are characteristic of the element and its state.

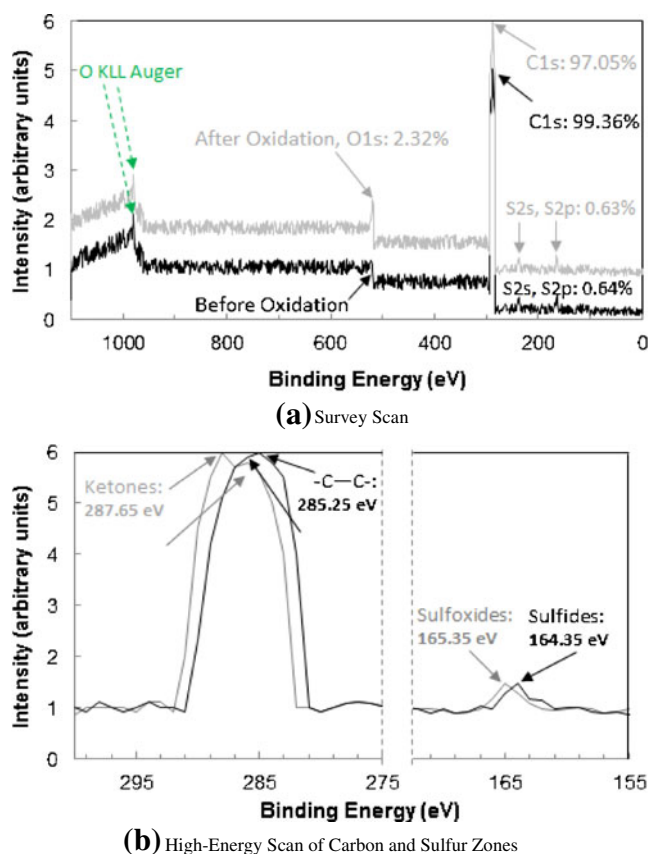
$$K_E = h\nu - E_b - \varphi \quad (9)$$

A Physical Electronics 5600 XPS setup was used, which provided the relative frequencies of binding energies of electrons. The binding energies were then used to identify the elements to which each peak corresponded, as elements of the same kind in different states and environments usually have different characteristic binding energies. Furthermore, comparing the areas under the peaks gave relative percentages of the elements detected in a sample. In preparing samples for XPS analysis, the asphalt samples were vacuumed at room temperature following the procedure established by Ruiz et al. [47]. The samples (in dry powders) were then pressed onto a piece of thin indium foil (0.1 mm

thick) as the sample substrate. The graphite tape was not used as sample substrate for the carbon-based asphalt to avoid peaks from the graphite tape, which would otherwise add to the carbon peak potentially skewing or overwhelming the data in XPS spectrum.

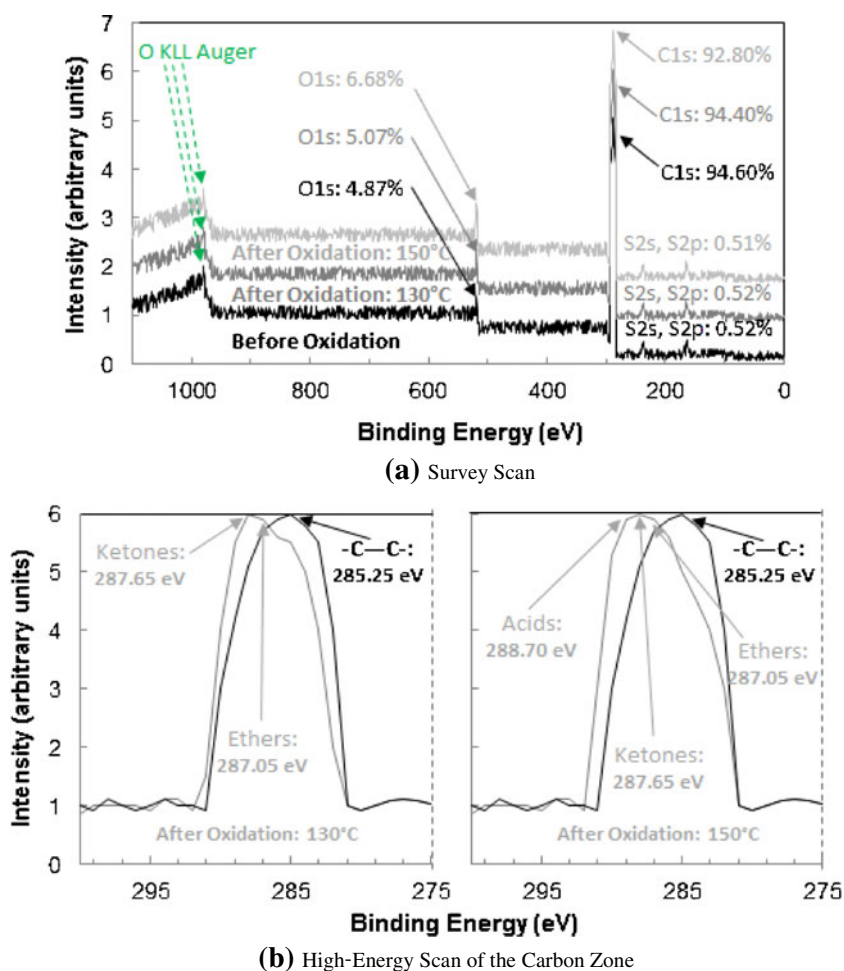
An initial survey XPS scan was conducted to identify the elements present in the unmodified and modified asphalt samples before and after oxidation (Figs. 3a and 4a), followed with a subsequent high-resolution scan of the peaks of interest, i.e., the carbon and sulfur in this study, to identify functional groups such as ketones, sulfoxides, ethers, and acids as observed in atomistic simulation (Figs. 3b and 4b). For the high-resolution scan, the computer software associated with the Physical Electronics 5600 XPS device detected the transform of sigma carbon–carbon single bonds (before oxidation) to the different carbon–oxygen bonds (after oxidation), and the transform of sulfides (before oxidation) to sulfoxides (after oxidation) at the carbon and sulfur peaks, as predicted by the ReaxFF-based atomistic models as shown in Figs. 1 and 2.

For the unmodified asphalt, the XPS spectra given in Fig. 3b clearly show the generation of ketones and sulfoxides during oxidation. For the asphalt modified with coniferyl-alcohol lignin, the XPS spectra given in Fig. 4b



**Fig. 3** XPS spectra of unmodified asphalt before and after oxidation, **a** survey scan; **b** high-energy scan of carbon and sulfur zones

**Fig. 4** XPS spectra of lignin-modified asphalt before and after oxidation, **a** survey scan; **b** high-energy scan of the carbon zone



show the generation of ketones, ethers, acids, and sulfoxides during oxidation. The quantitative determination of these functional groups in both unmodified and modified asphalts all well conform to the predictions from the ReaxFF-based atomistic models. Furthermore, the generations of functional groups during oxidation are plotted in Fig. 5 for both XPS measurements and atomistic predictions. The XPS measurements further validate the ReaxFF-based bulk asphalt model by showing close results in the amounts of newly generated ketones, ethers, acids, and sulfoxides. The slight difference between the experimental results and numerical predictions might come from the machine and/or operation errors related to XPS.

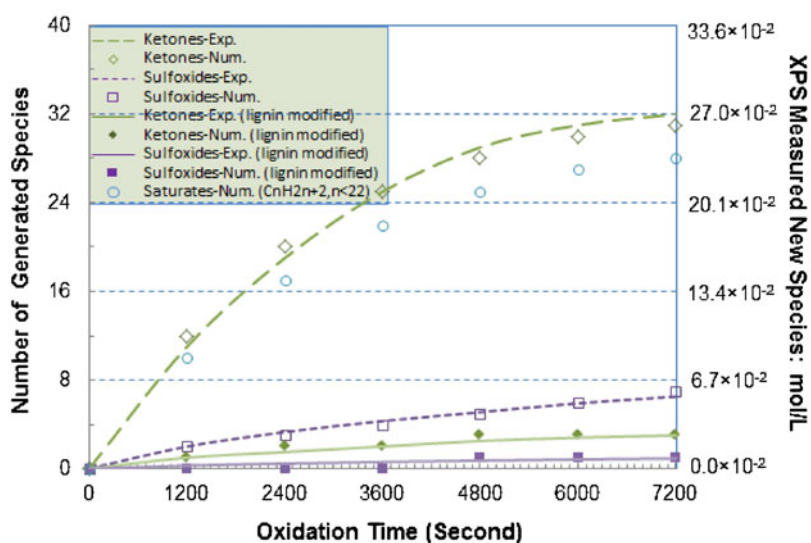
## Results and discussions

From the thermodynamic aspect of asphalt and lignin oxidation after two hours at 25 °C, 130 °C, and 150 °C (Fig. 1), asphalt molecules do not show signs of oxidation at 25 °C, however they do get oxidized at 130 and 150 °C; while the lignin molecules are not oxidized at 25 and 130 °C, however are oxidized at 150 °C during the simulation period. Also,

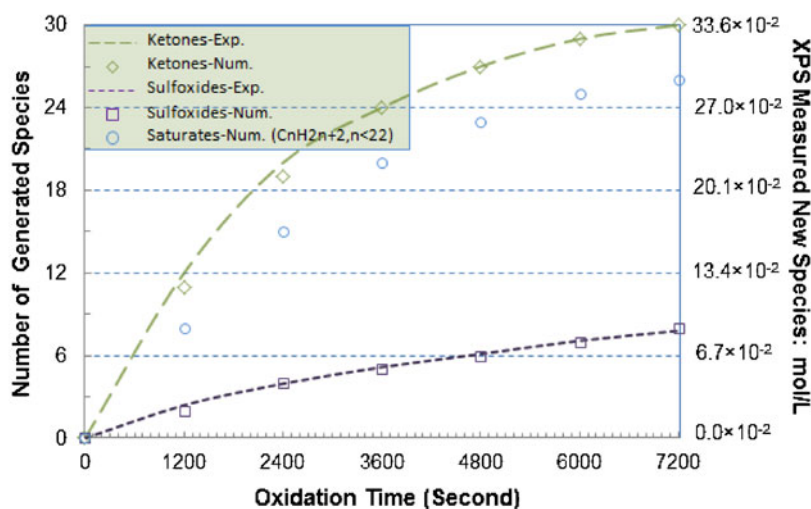
under the same oxidation condition (at 130 °C, 1 ATM) the different asphalt molecules oxidize at different rates and lead to different products. The carbon atoms in chain alkane, i.e., Saturate—C<sub>22</sub>H<sub>46</sub>, are quite resistant to oxidation; instead, the chain can break into shorter segments relatively easily. This could constitute an important mechanism for asphalt hardening as liquid portions of asphalt vaporize into air under general service conditions. The carbon atoms in aromatic (C<sub>12</sub>H<sub>12</sub>) show a partial level of oxidation, i.e., oxidized at the benzylic position, not the carbon atoms forming benzene rings, resulting in a ketone structure. Among the asphaltene molecules, i.e., the Asphaltene—C<sub>64</sub>H<sub>52</sub>S<sub>2</sub>, sulfoxidation occurs to one sulfur atom forming a sulfoxide (S=O), and ketonization occurs to one benzylic carbon atom. In asphaltenes, sulfoxidation seems to be easier than ketonization as the sulfoxide appears earlier than the ketone in the same asphaltene molecule. However, no aromatization was observed for the individual asphalt molecules.

The snapshot of the oxidation of the unmodified bulk asphalt as shown in Fig. 2b, displays two obvious phenomena: 1) generation of light-molecular-weight saturate molecules (with shorter chains than the two original saturates),

**Fig. 5** Experimental vs. numerical results of oxidized unmodified/modified bulk asphalt (two hours), **a** Generation of new functional groups at 130 °C; **b** generation of new functional groups at 150 °C



**(a)** Generation of New Functional Groups at 130°C



**(b)** Generation of New Functional Groups at 150°C

which tend to leave the bulk asphalt via diffusion; and 2) agglomeration of asphaltenes and aromatics as attracted by the oxygen-bearing functional groups. Some unbroken long saturates were also entangled with such agglomeration due to larger molecular weight and/or electrostatic forces. These two observations are in agreement with the phenomena of chain breaking of saturates, sulfoxidation, and ketonization as observed in the preceding thermodynamics models (on individual molecules). Probably, the two mechanisms contribute much to the oxidative hardening of asphalt.

Figures 2c and d show, respectively, the snapshots of the lignin-modified asphalt before and two hours after oxidation at 130 °C. At 130 °C the lignin does show effectiveness in anti-oxidation, which can be seen by comparing the levels of agglomeration in the bulk asphalt before (Fig. 2c) and after (Fig. 2d) oxidation. This anti-oxidation effect is owing to the scavenging action of lignin's phenolic structures on oxygen

containing free radicals, i.e., the ketones and sulfoxides formed in asphalt oxidation [17]. Phenolic structures are benzene rings with attached hydroxyl groups, which can form  $\pi$ -conjugation regions that promote the formation of donor-acceptor complex in modified asphalt. Such complexes act as catalysts or activators for scavenging the ketones and sulfoxides generated in asphalt oxidation [18, 48]. However, when the temperature is raised to 150 °C the lignin molecules started to become oxidized and generated vanillin and glycolaldehyde, and their scavenging action began to decrease. Further oxidation of lignin at 150 °C will lead to glycolic acid as observed in both atomistic simulation and XPS analysis. The increased level of agglomeration as lignin molecules started to become oxidized can be clearly seen in Fig. 2f in comparison to Fig. 2e.

The generated new species at 130 °C and 150 °C are summarized in Fig. 5. In unmodified asphalt the generation



rate of ketones seems to exceed that of sulfoxides due to the higher percentage of benzylic carbon atoms than sulfur atoms in asphalt. The generation rate of shorter chains shows a similar trend as ketones but at a slightly lower rate, both showing a higher generation rate than sulfoxides which might contribute more to the agglomeration of aged asphalt in the long run. When modified with lignin, the asphalt demonstrated a significantly slower oxidation rate at 130 °C than the unmodified asphalt. At 150 °C however, the generation rates of shorter-chain saturates and ketones are higher than those at 130 °C, also with a low rate of sulfoxide generation.

Based on this QC-based atomistic study, ketones and sulfoxides are the major oxidation products formed in oxidative aging of asphalt, which is in agreement to results of existing laboratory experiments such as by functional group analyses [5, 12]. Moreover, such oxidation products formed are consistently observed among field asphalts from different sources [37–40], and are in good agreement with the general oxidation chemistry of hydrocarbon and sulfur-containing molecules [44–46]. Ketones are a group of organic compounds carrying a carbonyl group, C=O, in which the carbon atom is bonded to two adjacent carbon atoms. Ketones are weak acids due to the  $\alpha$ -proton adjacent to the carbonyl group that are much more acidic compared to simple hydrocarbons, and can be removed by common bases such as HO<sup>-</sup> and RO<sup>-</sup>. Sulfoxides are another group of chemical compounds, containing a sulfinyl functional group, S=O, attached to two carbon atoms. The generation of ketones and sulfoxides are thermodynamically and kinetically favorable in general asphalt under the typical open-to-air conditions. Although the bond between sulfur and oxygen atoms differs from conventional double bonds like that between carbon and oxygen in ketones, sulfoxides and ketones are both polar, containing an electronegative oxygen atom producing a dipole in interaction or association with other dipoles or induced dipoles, thus both contributing to agglomeration of oxidized asphalt.

Lignins, when added in asphalt and not oxidized, will slow down the aging speed of asphalt. Also, usually added in solid powders, lignins can increase asphalt's stiffness. Lignins in general are more resistant to oxidation than asphaltenes and resins of asphalt under the same conditions. However, lignins do become oxidized at temperature of 150 °C and/or raised oxygen partial pressure, generating vanillin and glycolaldehyde for coniferyl-alcohol lignin. Sustained oxidation of the new species can lead to the generation of vanillic acid (from vanillin) and glycolic acid (from glycolaldehyde) that can be further oxidized to oxalic acid. When oxidized to low-molecular acids, methyl ethers, methyl ether esters, and methyl esters that have smaller sizes than oxidized asphaltenes and even naphthalenes, these new products help reduce the viscosity (as caused by ketones and sulfoxides in oxidized asphaltenes and naphthalenes) and recover the lost flowability and ductility of asphalt.

However the benefit owing to the smaller-size molecules is limited as can be seen from Fig. 5b, in which significant amounts of ketones and sulfoxides were generated from both asphalt and lignin molecules when the temperature is raised. Therefore, the anti-oxidation effect of lignins, if demonstrated, comes mainly from its scavenging actions at a non-oxidative temperature.

## Summary and conclusions

Based on a QC-based reactive force field re-evaluated for the C-H-O-S system, the oxidation of asphalt and the anti-oxidation mechanism of coniferyl-alcohol lignin are modeled and validated with XPS analyses. Important conclusions are made as follows.

1. Two distinct stages of asphalt aging can be identified based on the composition and structure of generated chemical species and their generation speeds. Asphalts initially exhibit a high chain-breaking trend and a high reactivity with oxygen, causing a rapid spurt in the formation of light-molecular-weight alkanes, ketones and sulfoxides. This spurt is followed by a slower rate of oxidation and hardening.
2. The oxidation of asphalt and lignin involves many stable radicals, and a number of intermediate chemicals that can only be observed at the atomic scale due to the high chemical instabilities of such intermediate products. Significant decomposition of saturates and evaporation of small-molecular-weight hydrocarbons were observed in the simulation. Ketones and sulfoxides account for most of the oxidative reactions in the simulated asphalt; however, the ratio of ketones to sulfoxides formed depends on sulfur content in asphalt. Therefore for the oxidative hardening of asphalt in typical service conditions, chain breaking of saturates, sulfoxidation, and ketonization at benzylic carbons are the major mechanisms.
3. The coniferyl-alcohol lignin can be used as antioxidant for petroleum asphalt, with the maximum radical-scavenging effectiveness achieved in a non-oxidative condition of the lignin (e.g., < 130 °C under 1 ATM oxygen partial pressure). This means that when added in asphalt the mixing temperature must be controlled to prevent lignin oxidation.

## References

1. McNichol D (2005) Paving the way: asphalt in America, 1st edn. National Asphalt Pavement Association, Lanham
2. Usmani AM (1997) Asphalt science and technology. Dekker, New York
3. Wess J, Olsen LD, Sweeney MH (2004) Asphalt (Bitumen). In: Concise International Chemical Assessment Document 59, World Health Organization, Geneva



4. Petersen JC, Branthaver JF, Robertson RE, Harnsberger PM, Duvall JJ, Ensley EK (1993) Effects of physicochemical factors on asphalt oxidation kinetics. *Transp Res Rec* 1391:1–10
5. Corbett LW (1969) Composition of asphalt based on generic fractionation using solvent deasphalting, elution-adsorption chromatography and densitometric characterization. *Anal Chem* 41:576–579
6. Davis TC, Petersen JC (1967) An inverse GLC study of asphalts used in the zaca-wigmore experimental test road. *Proc Assoc of Asph Paving Technol* 36:1–15
7. Plancher H, Green EL, Petersen JC (1976) Reduction of oxidative hardening of asphalts by treatment with hydrated lime: a mechanistic study. *Proc Assoc Asphalt Paving Technol* 45:1–24
8. Petersen JC (1998) A dual sequential mechanism for the oxidation of asphalts. *Pet Sci Technol* 16(9–10):1023–1059
9. Branthaver JF, Petersen JC, Robertson RE, Duvall JJ, Kim SS, Harnsberger PM, Mill T, Ensley EK, Barbour FA, Schabron JF (1993) Binder characterization and evaluation. In: Vol 2: chemistry report No SHRP-A-368 SHRP. National Research Council, Washington, DC
10. Petersen JC (1998) Asphalt aging: a dual oxidation mechanism and its interrelationships with asphalt composition and oxidative age hardening. *Transp Res Rec* 1638:47–55
11. Hveem FN, Zube E, Skog J (1959) Progress report on the zaca-wigmore experimental asphalt test project, special technical publication. *Am Soc Test Mater* 277:1–45
12. Petersen JC (1984) Chemical composition of asphalt as related to asphalt durability: state of the art. *Transp Res Rec* 999:13–30
13. Ruan Y, Davison RR, Glover CJ (2003) Oxidation and viscosity hardening of polymer-modified asphalts. *Energ Fuel* 17:991–998
14. Lucena MC, Soares SA, Soares JB (2004) Characterization of thermal behavior of polymer-modified asphalt. *Mat Res* 7:529–534
15. Bishara SW, Robertson RE, Mohoney D (2005) Lignin as an antioxidant: a limited study on asphalts frequency used on Kansas roads. The 42nd Peterson Asphalt Research Conference, Cheyenne, WY
16. Boerjan W, Ralph J, Baucher M (2003) Lignin bios. *Annu Rev Plant Biol* 54(1):519–549
17. Dizhbite T, Telysheva G, Jurkane V, Viesturs U (2004) Characterization of the radical scavenging activity of lignins-natural antioxidants. *Bioresour Technol* 95:309–317
18. Boeriu CG, Bravo D, Gosselink RJ, Van Dam JE (2004) Characterization of structure-dependent functional properties of lignin with infrared spectroscopy. *Ind Crop Prod* 20:205–218
19. Brink DL, Bicho JG, Merriman MM (1966) Oxidation degradation of wood III. In: lignin, structure and reactions. *Adv Chem Series* 59:177
20. Bryan CC (1954) Manufacture of Vanillin from Lignin. United States Patent 2692291
21. Pan T, van Duin ACT (2011) Steel surface passivation at a typical ambient condition: atomistic modeling and X-ray diffraction/reflectivity analyses. *Electrocatalysis* 2(4):307–316
22. Pan T, van Duin ACT (2011) Passivation of Steel Surface: An atomistic modeling approach aided with X-ray analyses. *Mater Lett* 65(21–22):3223–3226
23. Pan T (2011) Quantum chemistry-based study of iron oxidation at the iron-water interface: an X-ray analysis aided study. *Chem Phys Lett* 511(4–6):315–321
24. van Duin ACT, Dasgupta S, Lorant F, Goddard WA (2001) ReaxFF: a reactive force field for hydrocarbons. *J Phys Chem A* 105(41):9396–9409
25. Pan T, Xi Y (2011) Physicochemical nature of iron oxidation in a damp atmospheric condition. *Acta Metall Sin* 24(6):415–422
26. Pan T, Lu Y (2011) Quantum-chemistry based studying of rebar passivation in alkaline concrete environment. *Int J Electrochem Sci* 8
27. Parr RG, Yang W (1989) Density-functional theory of atoms and molecules. Oxford University Press, New York
28. Chenoweth K, van Duin ACT, Goddard WA (2008) ReaxFF reactive force field for molecular dynamics simulations of hydrocarbon oxidation. *J Phys Chem A* 112:1040–1053
29. Mortier WJ, Ghosh SK, Shankar S (1986) Electronegativity-equalization method for the calculation of atomic charges in molecules. *J Am Chem Soc* 108:4315–4320
30. Janssens GOA, Baekelandt BG, Toufar H, Mortier WJ, Schoonheydt RA (1995) Comparison of cluster and infinite crystal calculations on zeolites with the electronegativity equalization method (EEM). *J Phys Chem* 99:3251–3258
31. Njo SL, Fan J, van de Graaf B (1998) Extending and simplifying the electronegativity equalization method. *J Mol Catal A* 134:79–88
32. White RM, Mitten WR, Skog JB (1970) Fractional components of asphalt: compatibility and interchangeability of fractions produced from different asphalt. *Proc Assoc Asphalt Paving Technol* 39:498–531
33. Zhang L, Greenfield ML (2007) Relaxation time, diffusion, and viscosity analysis of model asphalt systems using molecular simulation. *J Chem Phys* 127:194502
34. Kowalewski I, Vandenbroucke M, Huc AY, Taylor MJ, Faulon JL (1996) Preliminary results on molecular modeling of asphaltenes using structure elucidation programs in conjunction with molecular simulation programs. *Energ Fuel* 10:97–107
35. Artok L, Su Y, Hirose Y, Hosokawa M, Murata S, Nomura M (1999) Structure and reactivity of petroleum-derived asphaltene. *Energ Fuel* 13:287–296
36. Groenzin H, Mullins OC (2000) Molecular size and structure of asphaltenes from various sources. *Energ Fuel* 14:677–684
37. Petersen JC, Plancher H, Miyake G (1983) Chemical reactivity and flow properties of asphalts modified by metal complex-induced reaction with atmospheric oxygen. *Proc Assoc Asphalt Paving Technol* 32:32–60
38. Shi X, Akin M, Pan T, Fay L, Yang Z (2009) Deicer impacts on pavement materials: introduction and recent developments. *Open Civ Eng J* 3:16–27
39. Pan T, He X, Shi X (2008) Laboratory investigation of acetate-based deicing/anti-icing agents deteriorating airfield asphalt concrete. *J Assoc Asphalt Paving Technol* 77:773–793
40. Griffen RL, Simpson WC, Miles TK (1959) Influence of composition of paving asphalts on viscosity, viscosity-temperature susceptibility, and durability. *J Chem Eng Data* 4:349–354
41. Storm DA, Edwards JC, DeCanio SJ, Sheu EY (1994) Molecular representations of Ratawi and Alaska north slope asphaltenes based on liquid- and solid-state NMR. *Energ Fuel* 8:561–566
42. Verlet L (1967) Computer ‘Experiments’ on classical fluids: i thermodynamical properties of lennard-jones molecules. *Phys Rev* 159(1):98–103
43. Berendsen HJC, Postma JPM, van Gunsteren W, DiNola A, Haak JR (1984) Molecular dynamics with coupling to an external bath. *J Chem Phys* 81:3684–3690
44. Gelius U, Heden RF, Hedman J, Lindberg BJ, Manne R, Nordberg R, Siegbahn K (1970) Molecular spectroscopy by means of ESCA III: carbon compounds. *Phys Scripta* 2(1–2):70–80
45. Kelemen SR, George GN, Gorbaty ML (1990) Direct determination and quantification of sulfur forms in heavy petroleum and coals: 1 the X-ray photoelectron spectroscopy (XPS) approach. *Fuel* 69:939–944
46. Lindberg BJ, Hamrin K, Johansson G, Gellius U, Fahlman A, Nordlind C, Siegbahn K (1970) Molecular spectroscopy by means of ESCA II: sulfur compounds, correlation of electron binding energy with structure. *Phys Scr* 1(5–6):288–298
47. Ruiz JM, Carden BM, Lena LJ, Vincent EJ, Escaller JC (1982) Determination of sulfur in asphalts by selective oxidation and photometric spectroscopy for chemical analysis. *Anal Chem* 54:688–691
48. Kuzina SI, Demidov SV, Brezgunov AY, Poluektiv OG, Grinberg OY, Dubinski AA, Mikhailov AI, Lebedev YS (1993) Study of free-radical centers in lignin with 20mm band ESR spectroscopy. *J Polym Sci A35(7):798–802*